

Crystal Structure of Cavansite Dehydrated at 220°C

BY ROMANO RINALDI,* J. J. PLUTH AND J. V. SMITH

Department of Geophysical Sciences, University of Chicago, Chicago, Ill. 60637, U.S.A.

(Received 20 November 1974; accepted 22 January 1975)

A single crystal of the new mineral cavansite, $\text{Ca}(\text{VO})(\text{Si}_4\text{O}_{10})\cdot 4\text{H}_2\text{O}$, from the type locality (Malheur County, Oregon) was dehydrated at $220 \pm 10^\circ\text{C}$ in a quartz capillary at $\sim 10^{-5}$ atm for 24 h. Intensity data from a four-circle diffractometer were refined anisotropically by least-squares calculations and Fourier techniques to $R=0.036$, $R_w=0.022$ in space group $Pcmm$. The cell dimensions change upon dehydration from $a=9.792$ (2), $b=13.644$ (3), $c=9.629$ (2) Å, $V=1286.5$ (3) Å³ to $a=9.368$ (2), $b=12.808$ (3), $c=9.550$ (2) Å, $V=1145.8$ (3) Å³. The 11% reduction of volume results mainly from removal of water between the silicate layers which lie perpendicular to **b**. The layers consist of four- and eight-membered rings of SiO_4 tetrahedra linked so that the sequence of tetrahedra around the eight-rings is $UUUDDDD$ (*U* up, *D* down). The layers are connected vertically (**b** direction) by V^{4+} cations in a square pyramidal coordination to give an infinite silicate-vanadyl complex. Replacement of each VO_5 group by two bridging oxygens gives the framework of the zeolite gismondine which has the same layers of four- and eight-membered rings but displays a fully expanded configuration. The Ca cations and the water molecules reside in the channels formed by the eight-rings and between the SiO_2 layers. At 220°C only one water molecule per Ca ion occurs in the structure. Removal of this last water molecule probably corresponds to the breakdown of the structure observed at $\sim 400^\circ\text{C}$. The vanadyl groups were found to have two orientations with the unshared oxygens pointing in opposite directions with a ratio of 10:1. Therefore there are two ideal structural models of cavansite with an infinite number of disordered intermediates.

Introduction

Cavansite and pentagonite dimorphs of $\text{Ca}(\text{VO})\text{Si}_4\text{O}_{10}\cdot 4\text{H}_2\text{O}$ were described recently as new minerals (Staples, Evans & Lindsay, 1973). Their structures consist of linked silicate tetrahedra bridged by vanadyl groups to yield an infinite framework enclosing Ca ions and water molecules (Evans, 1973). Because of possible analogies with zeolite molecular sieves, which have wide commercial applications, we have determined the structure of dehydrated cavansite: preliminary results were given by Rinaldi, Pluth & Smith (1974). A similar study of dehydrated pentagonite waits upon preparation of a suitable crystal.

We also investigated the relationships between the structures of cavansite and pentagonite and of other framework structures. As already mentioned by Evans (1973), replacement of the VO_5 group in cavansite by two bridging oxygens (or subtraction of VO_3) would produce a tetrahedral framework topologically identical with that of the zeolite gismondine (Fischer, 1963). Actually the structure of gismondine is expanded so that the eight-rings are nearly circular, as expected for a $UUDD$ -type structure of the flexible type (Smith & Rinaldi, 1962; Smith, 1968), whereas the structure of cavansite is contracted with near-elliptical rings. The same replacement of VO_5 from pentagonite generates a framework structure topologically identical with that of paracelsian. Here, however, pentagonite has an expanded configuration with nearly circular eight-

rings whereas the anhydrous paracelsian is contracted.

The topologic relations, with implications for new families of materials with zeolitic properties, are detailed elsewhere.

Experimental

A single crystal ($0.22 \times 0.040 \times 0.034$ mm, isosceles triangular prism) was inserted in a quartz capillary that had been pulled to achieve an internal diameter approximately equal to the small dimension of the crystal. The capillary walls were thinned to approximately 0.005 mm to minimize absorption of the X-rays. The capillary with crystal was evacuated at 10^{-5} Torr and kept at $220 \pm 10^\circ\text{C}$ for 24 h before sealing and cooling.

Two sets of Weissenberg X-ray photographs were taken before and after dehydration to check for permanent changes in the diffraction spectrum or crystal damage during dehydration. No changes were observed apart from a drastic reduction of the cell dimensions (11% in volume) from $a=9.792$ (2), $b=13.644$ (3), $c=9.629$ (2) Å, $V=1286.5$ (3) Å³ in the hydrated state (Evans, 1973), to $a=9.368$ (2), $b=12.808$ (3), $c=9.550$ (2) Å, $V=1145.8$ (3) Å³ in the dehydrated state. The cell dimensions in the dehydrated form were determined by the least-squares refinement of 23 high 2θ values (Burnham, 1962) measured on a Picker FACS-1 diffractometer at room temperature and obtained by averaging four half-height peak settings (plus and minus 2θ). No change in the space group was observed upon dehydration. The extinction conditions are $0kl$ present with $l=2n$, $h0l$ present in all

* Present address: Istituto di Mineralogia e Petrologia, Università di Modena, I-41100 Modena, Italy.

orders, and $hk0$ present with $h+k=2n$; possible space groups are $Pcmm$ or $Pc2_1n$. The centrosymmetric space group was adopted as proposed by Evans (1973).

The chemical analysis of cavansite reported by Evans (1973) yielded stoichiometric $\text{Ca}(\text{VO})(\text{Si}_4\text{O}_{10}) \cdot 4\text{H}_2\text{O}$. On the basis of population refinement, the dehydrated form at 220°C retains one residual H_2O .

Intensity data were collected at room temperature on a Picker FACS-1 automated single-crystal diffractometer with θ - 2θ scans; 2841 diffractions (four equivalent sets) were measured $[(\sin \theta/\lambda)_{\max}=0.497]$ using $\text{Cu } K\alpha$ radiation ($\lambda=1.5418$). After averaging, the resulting 571 independent diffractions with $F \leq 2\sigma_F$ were used in the refinement.

The estimated errors in the intensities (σ_I) were calculated by: $\sigma_I=[S+t^2B+k^2(S+tB)^2]^{1/2}$ where S =peak scan counts, B =total background counts, t =ratio of peak to background observation times, k =instability constant (0.01).

The equivalent diffractions were averaged using:

$$I = \sum_i (I_i/\sigma_i^2) / \sum_i (1/\sigma_i^2),$$

$$\bar{\sigma}_I = [1/\sum_i (1/\sigma_i^2)]^{1/2}$$

where I_i and σ_i are the intensity and the standard deviation of the i th equivalent diffraction. The intensity data were corrected for Lorentz and polarization effects, but no absorption correction was applied. The linear absorption coefficient for the crystal alone (not

including the capillary) was $\mu=156 \text{ cm}^{-1}$, an absorption correction test revealed a maximum error in the structure factors of only 3% due to the very small size of the crystal. The approximations in calculating the absorption corrections would therefore introduce errors of the same order of magnitude as the corrections to be made.

The σ_I 's were converted to the estimated errors in the relative structure factors (σ_F) by $\sigma_F=[(I+\bar{\sigma}_I)/Lp]^{1/2} - (I/Lp)^{1/2}$ with Lp =Lorentz and polarization factors.

Structure refinement

The atomic coordinates given for hydrated cavansite, excluding water molecules (Evans, 1973), were used to start the refinement. Isotropic refinement converged from a starting residual $R=0.41$ to a final $R=0.091$. A difference Fourier synthesis revealed a peak ($4.6 \text{ e } \text{\AA}^{-3}$) approximately in the middle of the large channel which was assigned to water molecule $W(1)$. Isotropic least-square refinement varying the population parameter of $W(1)$ yielded $R=0.056$. The population parameter of $W(1)$ remained at unity and was therefore fixed at this point. A difference Fourier synthesis at this stage revealed a residual peak ($2.4 \text{ e } \text{\AA}^{-3}$) in the same plane as V but located about 1 \AA from it. This suggested occupancy of another position near V(1) with a population factor of 0.1. Such a position would coordinate to the same framework oxygens as V(1) but to a different apical oxygen in the VO_5 group. This

Table 1. Positional, thermal and population parameters

	Equipoint	x/a	y/b	z/c	B (\AA)*	Population
Ca	4(c)	0.0597 (2)	$\frac{1}{4}$	0.3824 (2)	1.65 (5)	4
V(1)	4(c)	0.1144 (2)	$\frac{1}{4}$	0.0400 (2)	1.63 (8)	3.70 (4)
V(2)	4(c)	0.2063 (22)	$\frac{1}{4}$	0.0919 (24)	3.87 (86)	0.43 (4)
Si(1)	8(d)	0.0803 (2)	0.0173 (1)	0.1926 (2)	1.53 (4)	8
Si(2)	8(d)	0.2871 (1)	0.0334 (1)	0.4178 (2)	1.44 (4)	8
O(1)	8(d)	0.0770 (3)	0.1432 (2)	0.1887 (3)	1.87 (10)	8
O(2)	8(d)	0.2464 (4)	0.1506 (2)	0.4596 (4)	1.85 (9)	8
O(3)	8(d)	0.4217 (3)	0.0302 (3)	0.3124 (3)	1.91 (9)	8
O(4)	8(d)	0.1710 (3)	-0.0289 (3)	0.0596 (3)	1.69 (9)	8
O(5)	8(d)	0.1541 (3)	-0.0216 (3)	0.3393 (3)	1.58 (9)	8
O(6)	4(c)	0.5200 (6)	$\frac{1}{4}$	0.4419 (6)	2.97 (26)	3.73 (9)
O(7)	4(c)	0.3761 (87)	$\frac{1}{4}$	0.1665 (56)	7.34 (3.8)	0.39 (10)
$W(1)$	4(c)	0.3199 (7)	$-\frac{1}{4}$	0.0608 (9)	8.37 (33)	4

* B 's from last cycle of isotropic refinement.

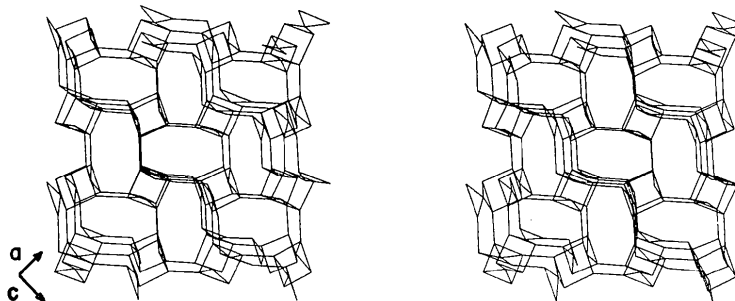


Fig. 1. Cavansite framework structure looking down b ; the nodes correspond to the positions of Si and V atoms; oxygen atoms lie approximately at the midpoints of the lines between nodes.

second V position was supported by the presence of a very small peak ($0.6 \text{ e } \text{Å}^{-3}$) corresponding to the position of the predicted apical oxygen. Again the indicated population factor was near 0.1. Isotropic least-squares refinement converged to $R=0.040$. The population parameters of these two new atomic positions V(2) and O(7) and those of V(1) and O(6) were varied during the refinement and refined very close to 0.1 and 0.9. Population parameters were all fixed at this point and the refinement was completed using anisotropic thermal parameters. The final cycle minimized $\sum w||F_o| - |F_c||^2$ with $w=(1/\sigma_F)^2$. The maximum shift ($\sim 0.4\sigma$) appeared in the thermal parameter of O(7), probably because of its very low population. The temperature factor of O(7) was also non-positive definite at the end of the refinement. The final residual indices were $R=0.036$, $R_w=0.022$, $S=1.95$ where:

$$R = \frac{\sum ||F_o| - |F_c||}{\sum |F_o|};$$

$$R_w = \frac{[\sum w||F_o| - |F_c||^2 / \sum w|F_o|^2]^{1/2}}{S};$$

$$S = \frac{[\sum w||F_o| - |F_c||^2 / (n_o - n_p)]^{1/2}}{S};$$

with n_o = number of diffractions, n_p = number of parameters.

Atomic scattering factors (Mann, 1968) were used for Ca^{2+} , V^{4+} , Si^{2+} and O^- (for which V^{4+} was interpolated between V^{3+} and V^{5+} and Si^{2+} between Si and Si^{4+}). Anomalous scattering corrections (Cromer & Liberman, 1970) were applied to all atoms. The final model was checked by difference-Fourier synthesis. No significant peaks were observed in the vicinity of any of the atomic positions. The maximum residual electron density was $0.4 \text{ e } \text{Å}^{-3}$.

The results are given in Table 1 (positional, thermal and population parameters), Table 2* (structure factors), Table 3 (anisotropic thermal parameters), Table 4* (r.m.s. components and directions of thermal dis-

* Tables 2 and 4 have been deposited with the British Library Lending Division as Supplementary Publication No. SUP 30895 (6 pp.). Copies may be obtained through The Executive Secretary, International Union of Crystallography, 13 White Friars, Chester CH1 1NZ, England.

Table 3. *Anisotropic thermal parameters*

The anisotropic temperature factor is in the form

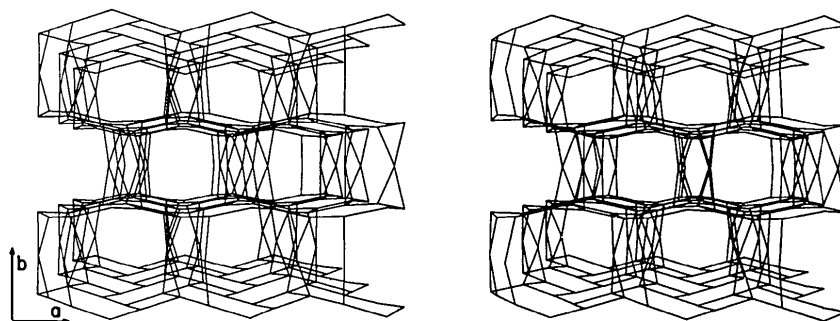
$$\exp \left[- \sum_{j=1}^3 \sum_{i=1}^3 \beta_{ij} h_i h_j \right]. \text{ The } \beta \text{ values are multiplied by } 10^4.$$

	β_{11}	β_{22}	β_{33}	β_{12}	β_{13}	β_{23}
Ca	50 (2)	27 (1)	51 (2)	0	0 (2)	0
V(1)	46 (2)	25 (1)	46 (3)	0	2 (2)	0
V(2)	116 (31)	42 (14)	162 (37)	0	4 (29)	0
Si(1)	51 (2)	26 (1)	38 (2)	2 (1)	0 (2)	1 (1)
Si(2)	39 (2)	23 (1)	44 (2)	1 (1)	-6 (2)	0 (1)
O(1)	66 (5)	22 (3)	43 (5)	2 (3)	6 (4)	0 (3)
O(2)	59 (4)	21 (2)	51 (5)	6 (4)	-6 (4)	-4 (3)
O(3)	34 (5)	36 (3)	45 (5)	7 (4)	0 (4)	3 (4)
O(4)	50 (5)	22 (3)	50 (6)	-3 (3)	-3 (4)	2 (3)
O(5)	43 (5)	25 (3)	33 (5)	-6 (3)	0 (4)	3 (3)
O(6)	70 (9)	39 (5)	104 (10)	0	0 (8)	0
O(7)	505 (201)	119 (78)	29 (91)	0	-237 (117)	0
W(1)	141 (13)	145 (9)	332 (19)	0	-85 (13)	0

Table 5. *Comparison of bond distances (Å) and angles (°) for hydrated and dehydrated cavansite*

SiO ₄ tetrahedra	Hydrated	Dehydrated
Si(1)-O(1)	1.611 (14)	1.614 (3)
Si(1)-O(3)	1.633 (13)	1.606 (3)
Si(1)-O(4)	1.651 (13)	1.640 (4)
Si(1)-O(5)	1.645 (15)	1.639 (3)
Average	1.635	1.625
O(1)-Si(1)-O(3)	113.4 (8)	111.2 (2)
O(1)-Si(1)-O(4)	111.5 (7)	110.6 (2)
O(1)-Si(1)-O(5)	113.5 (8)	109.4 (2)
O(3)-Si(1)-O(4)	107.6 (7)	108.6 (2)
O(3)-Si(1)-O(5)	103.3 (7)	107.5 (2)
O(4)-Si(1)-O(5)	107.1 (7)	109.5 (2)
Si(2)-O(2)	1.613 (16)	1.600 (3)
Si(2)-O(3)	1.611 (13)	1.614 (3)
Si(2)-O(4)	1.630 (14)	1.620 (3)
Si(2)-O(5)	1.623 (15)	1.616 (3)
Average	1.619	1.613
O(2)-Si(2)-O(3)	111.4 (8)	111.5 (2)
O(2)-Si(2)-O(4)	111.2 (7)	108.2 (2)
O(2)-Si(2)-O(5)	110.8 (8)	109.9 (2)
O(3)-Si(2)-O(4)	109.8 (7)	108.6 (2)
O(3)-Si(2)-O(5)	107.3 (7)	107.6 (2)
O(4)-Si(2)-O(5)	106.2 (7)	111.1 (2)
Oxygen links		
Si(1)-O(3)-Si(2)	136.4 (8)	138.7 (2)
Si(1)-O(4)-Si(2)	126.5 (9)	126.5 (2)
Si(1)-O(5)-Si(2)	129.1 (9)	126.1 (2)
Si(1)-O(1)-V(1)	135.4 (7)	134.1 (2)
Si(2)-O(2)-V(1)	127.9 (9)	122.9 (2)
Si(1)-O(1)-V(2)		131.8 (4)
Si(2)-O(2)-V(2)		139.5 (5)
VO ₅ square pyramids		
2V(1)-O(1)	1.976 (12)	2.002 (3)
2V(1)-O(2)	1.973 (14)	1.977 (4)
V(1)-O(6)	1.597 (22)	1.569 (6)
V(1)-O(8) (H ₂ O)*	2.887 (33)	
2V(2)-O(1)		2.047 (14)
2V(2)-O(2)		1.847 (15)
V(2)-O(7)		1.743 (70)
2O(1)-V(1)-O(6)	104.6 (8)	106.4 (2)
2O(2)-V(1)-O(6)	104.7 (8)	107.3 (2)
2O(1)-V(1)-O(2)	90.3 (6)	87.2 (1)
O(1)-V(1)-O(1)	86.6 (7)	86.1 (2)
O(2)-V(1)-O(2)	78.2 (4)	80.1 (2)
2O(1)-V(2)-O(7)		110.8 (19)
2O(2)-V(2)-O(7)		93.5 (18)
2O(1)-V(2)-O(2)		89.5 (3)
O(1)-V(2)-O(1)		83.8 (7)
O(2)-V(2)-O(2)		87.1 (9)
Ca coordination		
2Ca-O(1)	2.385 (12)	2.285 (4)
2Ca-O(2)	2.433 (15)	2.306 (3)
Ca-W(1) (H ₂ O)		2.312 (6)
Ca-O(7) (H ₂ O)*	2.392 (17)	
Ca-O(8) (H ₂ O)*	2.516 (21)	
Ca-O(9) (H ₂ O)*	2.844 (43)	
Hydrogen bonds		
W(1)-O(6)		2.809 (9)
O(7)-O(1)*	2.86 (2)	
O(7)-O(8)*	2.89 (4)	
O(7)-O(9)*	3.00 (3)	

* O(7), O(8), O(9) were water molecules in Evans (1973) notation.

Fig. 2. Cavansite framework structure looking down *c*.

placement), and Table 5 (interatomic distances and angles). Interatomic distances and angles were calculated using the computer program *ORFFE* (Busing, Martin & Levy, 1964). The figures were obtained from *ORTEP* plots (Johnson, 1965).

Discussion

The framework of cavansite is formed by silicate layers of four- and eight-membered rings of tetrahedra

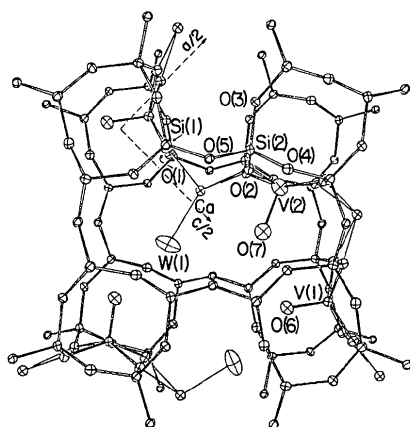


Fig. 3. The structure of dehydrated cavansite; Ca atoms have line bonds; origin of coordinate system at $b = \frac{1}{4}$; 25% ellipsoids of vibration; V(2) and O(7) occupy one of the four V positions; O(7) is represented by its isotropic ellipsoid of vibration.

connected vertically (*b* direction) by V^{4+} cations in a square pyramidal coordination (Figs. 1 and 2). (The framework oxygens and apical oxygen of the square pyramid are not shown in Figs. 1 and 2, but are in Fig. 4.) The tetrahedra of the silicate layers have the *UUUDDDD* sequence characteristic of the zeolite gismondine, and the structure is of the flexible type. Such a framework can undergo adjustments in order to accommodate different kinds and quantities of sorbates. Imagine that one of the four-rings in Fig. 1 rotates in the plane of the layers. Such a rotation propagates throughout the structure, thereby expanding or contracting the free diameter of the channels formed by the eight-rings. Oxygen atoms act as pivots during this imaginary rotation. In gismondine the eight-rings are nearly circular (axial ratio 1.1) whereas in cavansite they are elliptical with axial ratios of 1.7 and 2.2 in the hydrated and dehydrated forms, respectively. In the dehydrated state the minimum free diameter of the channels formed by the eight-rings, calculated from O(5) to O(5), is 1.55 Å, assuming an effective radius for oxygen of 1.35 Å. These channels, however, are obstructed by the Ca atom and residual H_2O .

The presence of V as bridging element between silicate layers produces another system of open channels running parallel to the *ac* plane (Fig. 2). This suggests the possibility of having a series of compounds in which other transition metals could assume the same role within a silicate-type structure thereby providing a range of different pore sizes and (possibly) catalytic activities suitable for various uses in molecular sieve

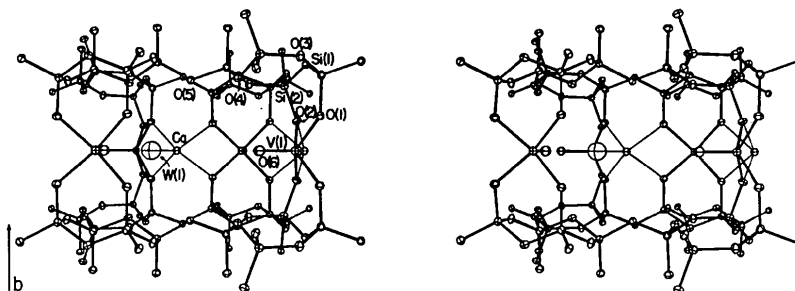


Fig. 4. The structure of dehydrated cavansite looking down the *ca* diagonal; same portion of framework as in Fig. 3 less V(2) and O(7); 25% ellipsoids of vibration.

technology. The largest channels in the structure occur parallel to the *c* direction (Fig. 2) with a minimum free diameter of 3.3 Å in the hydrated state and 3.2 Å in the dehydrated form [calculated from O(1) to O(6)].

The vanadyl groups were found to occur with two different orientations throughout the structure with the apex of the pyramid pointing the opposite direction in 10% of the sites (Fig. 3). The 'flipping' of 1 out of 10 of the V's occurs randomly in the structure and the X-ray data give no indication of ordering between the two possible orientations. Whether the less frequent kind of orientation occurs as a result of dehydration is being investigated by collection of further X-ray data. It would be hard to detect in the hydrated state, because water molecules lie near the positions occupied by V(2) and O(7); however, the one-site model for the hydrated form yielded $R=11\%$ versus $R=4\%$ for the two-site model of the dehydrated form. Because the two orientations are topologically distinct, there are two ideal structural models of cavansite with an infinite number of disordered intermediates.

The V(1) coordination polyhedron (Figs. 4 and 5) undergoes slight changes upon dehydration. The distances remain nearly constant but the O–V(1)–O angles change in the sense of making the V(1) square pyramids protrude further into the large channels, to accommodate for the shortening of the *b* repeat period. The V(1)–O(6) distance is shorter than the other V(1)–O bonds being an oxide bond. The coordination of V(2) is also regular, although with larger errors associated with the larger thermal parameters (Table 5).

Upon dehydration Ca moves closer to the framework oxygens O(1) and O(2) and it also pulls the water molecule W(1) to a closer coordination distance of 2.3 Å (Fig. 6). The average Ca–O coordination distance changes from 2.43 Å in the hydrated form to 2.30 Å in the dehydrated one. This latter distance is short compared with typical Ca–O distances in silicates (usually about 2.4 Å). Perhaps the shortening results from the lower coordination (five in dehydrated cavansite vs typically six to seven in silicates).

The coordination polyhedron of Ca is very similar to that of V, being bonded to four framework oxygens and one residual water molecule that projects into the large channels. A hydrogen bond possibly exists between W(1) and O(6) (Table 5). In the hydrated state the Ca coordination was approximately trigonal prismatic.

Breakdown of the structure, observed at approximately 400°C by high-temperature powder diffraction experiment (Evans, 1974, personal communication), probably results from removal of the last water molecule.

Experiments on the ion exchange properties of cavansite are desirable in order to establish its zeolitic properties and the role of Ca in the structure.

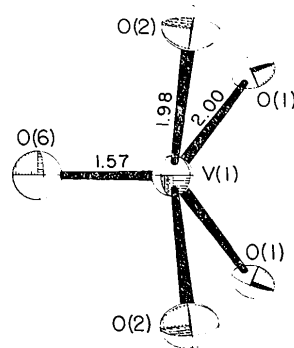


Fig. 5. V(1) coordination polyhedron; distances in Å; 50% ellipsoids of vibration.

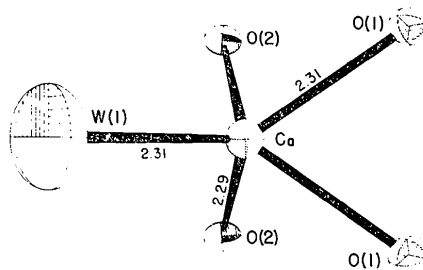


Fig. 6. Ca coordination polyhedron; distances in Å units; 50% ellipsoids of vibration.

We thank D. W. Breck for pointing out the possible relation between cavansite and zeolites; M. Groben for providing the samples; H. T. Evans for X-ray data on dehydration; the donors of the Petroleum Research Fund administered by the American Chemical Society for grant-in-aid 6276 AC2 and Union Carbide Corporation for financial aid; and the Materials Research Laboratory financed by the National Science Foundation for general support.

References

- BURNHAM, C. W. (1962). *Carnegie Inst. Wash. Yearb.* **61**, 132–135.
 BUSING, W. R., MARTIN, K. O. & LEVY, H. A. (1964). *ORFFE*. Oak Ridge National Laboratory Report ORNL-TM-306.
 CROMER, D. T. & LIBERMAN, D. (1970). *J. Chem. Phys.* **53**, 1891–1898.
 EVANS, H. T. JR (1973). *Amer. Min.* **58**, 412–424.
 FISCHER, K. (1963). *Amer. Min.* **48**, 664–672.
 JOHNSON, C. K. (1965). *ORTEP*. Oak Ridge National Laboratory Report ORNL-3794.
 MANN, B. (1968). *Acta Cryst.* **A24**, 321–324.
 RINALDI, R., PLUTH, J. J. & SMITH, J. V. (1974). *Amer. Cryst. Assoc. Ser.* **2**, 2, 273.
 SMITH, J. V. (1968). *Miner. Mag.* **36**, 640–642.
 SMITH, J. V. & RINALDI, F. (1962). *Miner. Mag.* **33**, 202–212.
 STAPLES, L. W., EVANS, H. T. JR & LINDSAY, J. R. (1973). *Amer. Min.* **58**, 405–411.